

Spatial-temporal Correlation Analyses of Global Burned Surface Time Series from Remote Sensing data (1982-1999)

C. Carmona-Moreno^{a,*}, A. Belward^a, Ph. Caperan^a, A. Hartley^a, J.P. Malingreau^b, M. Antonovskiy^c, V. Buchshtaber^d, V. Pivovarov^d

^a European Commission, DG Joint Research Centre – (cesar.carmona-moreno, alan.belward, philippe.caperan, andrew.hartley)@jrc.it

^b European Commission, DG Joint Research Centre – Jean-Paul.Malingreau@cec.eu.int

^c Institute of Global Climate and Ecology. 107258, Moscow, st. Glebovskaya 20-b. Russia

^d National Russian Research Institute of Physical-Technical and Radiotechnical Measurements. 141570, Moscow region, Solnechnogorsky raion, p.Mendeleevo, Russia

Abstract – Daily global observations from the Advanced Very High Resolution Radiometers (AVHRR) on the series of meteorological satellites operated by the National Oceanic and Atmospheric Administration (NOAA) between 1982 and 1999 (17 years) were used to generate a new weekly global burnt surface product at a resolution of 8km. Comparison with independently available information on fire locations and timing suggest that whilst the time-series cannot yet be used to make accuracy and quantitative estimates of global burnt area, it does provide a reliable estimate of changes in location, season and interannual variability of burning on the global scale (Carmona-Moreno et al., 2005.a).

This paper deals with the connection analysis of this time series and “El Niño” Southern Oscillation (ENSO) events. The spatial-temporal inter-correlation analyses show likely connections between both phenomena at global scale during the period considered even if these results need to be confirmed with longer time series (>40 years) of data.

Keywords: Global Fire Dynamics, Global Burnt Surfaces time series, NOAA-AVHRR GAC 8km time series, ENSO 1-2 and 3.4 indices.

1. INTRODUCTION

On a global scale, biomass burning activity is driven by climate/weather and has direct consequences on atmospheric chemistry (Malingreau et al., 1995; Tucker et al., 1986; Sellers et al., 1994; Belward et al., 1995; Crutzen et al., 1979). This process loads atmosphere with nitrogen oxides, carbon monoxide, black and organic carbon, mineral ash and volatile organic compounds, in addition to greenhouse gases such as nitrous oxide, carbon dioxide, and methane. Biomass burning thus contributes to air pollution, global warming, and the formation of acid rain. Therefore, fire activity could be considered as an indicator of the global climate dynamics.

In this perspective, regular monitoring of global burnt surface areas play an important role for the scientific community: first, to identify geographical areas affected by the global fire activity, establishing variability of the fire occurrence probability and frequencies (fire activity seasonality variations); and, second, to estimate the spatial distribution from burnt surfaces, atmospheric CO₂ – CO emissions, their inter-relationships and inter-variability.

The works of (Seiler and Crutzen, 1980), (Hao and Liu, 1994) and (FAO, 2001) are pioneer and alternative studies in this domain offering global estimates of burnt areas using national and international statistics. Remote sensing offers a unique opportunity to study and characterize the spatial-temporal dynamics of this phenomenon at global scale in a systematic and operational way (Malingreau et al., 1995; Innes et al., 2000). So far, little is known about burnt surfaces from remote sensing at global or continental scale and relatively little work has dealt with this issue at that level (Moreno-Ruiz et al., 1999; Dwyer et al., 2000; Barbosa et al., 1999; Arino et al., 2001). In this way, both Dwyer et al., 2000 and Arino et al., 2001 have listed global inventories of active fires. Dwyer et al., 2000 made it on the basis of a limited number of NOAA-AVHRR remote sensing data (from April 1992 to March 1993) with 1.1 by 1.1 km² of resolution; and, Arino et al., 2001 worked using ATSR satellite images from July 1996 to February 2002.

A new weekly satellite Earth Observation product called Global Burnt Surface Map (GBS) appears as an opportunity to better understand the global fire activity phenomenon (Moreno et al., 1999; Carmona-Moreno et al., 2005.a). This product is obtained from the daily NOAA-AVHRR GAC 8km data set (1982-1999). Carmona-Moreno et al., 2005.a-b introduce this new time series and characterize fire activity in both northern and southern hemispheres on the basis of average seasonal cycle and inter-annual variability. Fire seasonality and fire distribution datasets have been combined to provide gridded maps at 0.5 degree resolution documenting the probability of fire occurring in any given season for any location.

The purpose of this paper is to establish inter-correlations between GBS time series and El Niño Southern Oscillation (ENSO) 1-2 and 3.4 indices (table A) for the period considered here. ENSO has been associated with regional extremes in precipitation and temperature (Ropolewski and Halper, 1996) and in many cases, ENSO is supposed to correlate with exceptional fire events at regional scale (Swetnam and Betancourt, 1990). The aim of this paper is to show through correlation analyses – GBS and ENSO indices – the tele-connection between these phenomena at global scale during the period of time considered here.

The total amount of burnt surface per week is assumed as a surrogate of the fire activity as far as it can be considered that the larger the amount of burnt surface, the more important the fire activity is.

* Corresponding author.

** We wish to thanks the NASA-GODDARD DAAC for providing with NOAA-AVHRR 8km data.

2. DATA AND METHODS

2.1 NOAA-AVHRR GAC 8km data

The processor on board the satellite samples the real-time NOAA-AVHRR-LAC 1km resolution data to produce reduced resolution NOAA-AVHRR GAC data. Four out of every five samples along the scan line are used to compute one average value, and the data from only every third scan line are processed. As a result, the spatial resolution of GAC data near the subpoint is actually 1.1 km by 4km with a 3km gap between pixels across the scan line. A NOAA-AVHRR GAC image is then finally projected and resampled to 8km.

At this point, AVHRR-GAC images can be considered as the result of a systematic sampling strategy of AVHRR-LAC images. In this way as shown in (Carmona-Moreno et al., 2005.b) AVHRR GAC images are representative samplings of the original AVHRR-LAC images and as such only qualitative comparisons and trends can be deduced from them.

The burnt surface detection algorithm implemented for obtaining burnt surface maps uses daily NOAA-AVHRR 8km remote sensing data based on a weekly composite data set. The algorithm is an extension of (Barbosa et al., 1999) which is based on a multi-temporal and multi-spectral analysis with local thresholds.

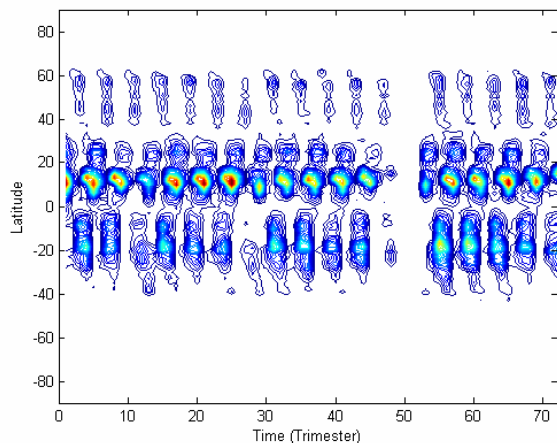


Figure 1. Spatial-temporal distribution of the GBS time series (1982-1999). 1994 data (trimesters: 48-52) are missing because of a crash of the satellite that year (Carmona-Moreno et al., 2005.a).

From this perspective, Global Burned Surfaces (GBS) time series has been developed for global fire activity behaviour analysis and research purposes, but caution should be exercised when interpreting the GBS time series on a quantitative basis. In this way, fire and burnt surfaces presenting high spatial variability like fires in gallery forests, “small” extensions of fires (<1500 ha), dark soils (some over-estimations has been detected in this product even if these errors have been minimized by the temporal and automatic detection analysis), under-story forest fires and low temperature peat fires (these important sources of CO cannot be detected by this algorithm) are errors that have not been considered, or underrepresented, by this data-set. Ever-cloudy areas (in boreal and some tropical regions, mainly) presented also some detection problems. Further information about omission and commission errors can be found in (Carmona-Moreno et al.,

2005.a). In this last work, (Carmona-Moreno et al., 2005.a) introduced a new representation of the variogram of the GBS time series modelled by a gridding method using an exponential fitting curve. Figure 1 shows the spatial-temporal structure of the GBS data distributed by latitudes ($90^{\circ}\text{S} - 0 - 90^{\circ}\text{N}$) and trimester periods (0 – 72 trimesters from 1982 to 1999).

We see in this figure that the global fire activity (measured as the extension of the burned surfaces detected by satellite data) occurs mainly (the most quantities of surfaces affected by fire) in the tropics ($20^{\circ}\text{S}-0^{\circ}-20^{\circ}\text{N}$) with “secondary” latitude regions (less quantities of surfaces affected by fire): ($20^{\circ}\text{N} -30^{\circ}\text{N}$) corresponding to Southern of North America, Mediterranean area, Mongolia, Central and North of China; and, finally, the boreal areas ($50^{\circ}\text{N} -75^{\circ}\text{N}$) corresponding with Canada and Russia.

2.2 ENSO Index time series

ENSO is a natural coupled cycle in the ocean-atmospheric system. As defined by the Scientific Committee on Oceanic Research (SCOR), ENSO is “the presence of anomalously warm water along the coast of Ecuador and Peru as far south as Lima (12°S) where the sea surface temperature anomaly (SST) exceeds one standard deviation for at least four consecutive months at three or more of five coastal stations (Talara, Puerto Chicama, Chimbote, Isla Don Martin and Callao)”. Therefore, ENSO is often measured by indices based on regional sea surface temperature (SST) anomalies in the tropical Pacific ocean. ENSO has three phases: warm tropical Pacific SSTs (El Niño), cold tropical Pacific SSTs (La Niña), and near neutral conditions. Figure 2 shows the two regional ENSO indices used in this work. Both regions are defined in table A. Positive values correspond with an El Niño events and negative values with La Niña.

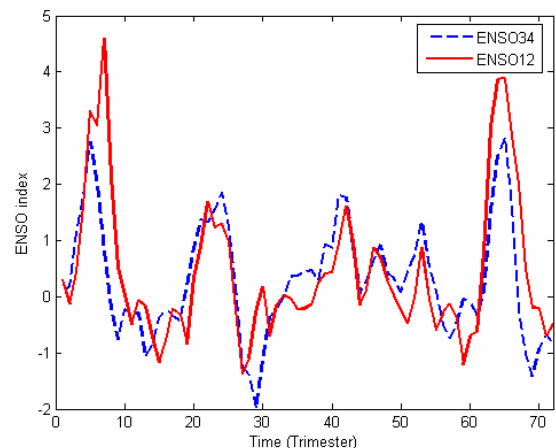


Figure 2. ENSO 3.4 and ENSO 1-2 indices.

Timing plays a role in which ENSO characteristics are best captured by the ENSO indices. The ENSO 3.4 index captures the ENSO event near its onset in the late summer. On another side, ENSO 1-2 best captures the events in the winter when ENSO events usually peak. ENSO 1-2 index is recognised to be influenced by the proximity of the continent and in this way it has differences in response to actual ENSO events (Hanley et al., 2003). This last paper points out that ENSO 3.4 index is more sensitive to La Niña events than ENSO 1-2 index. This could be a

source of noise in correlation with GBS time series as we will see later.

In this work, we have correlated both regional ENSO indices time series with the spatial-temporal GBS time series (one linear unidimensional correlation per latitude value). Figures 3 and 4 show the bidimensional plane of the inter-correlation (unbiased) results between both phenomena. The contour lines are associated to the correlation coefficients: the closer the contour line, the higher the correlation value is. Maximum values of the inter-correlation peaks show a spatial-temporal connection between both signals. In these figures, the *trimester shift* axe shows the time shift existing between both phenomena as measured by the linear correlation (unbiased), and the *latitude* axe shows the spatial distribution by degree of latitude.

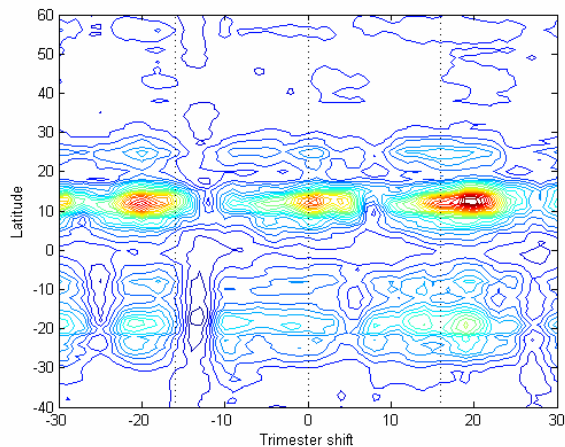


Figure 3. Spatial-temporal inter-correlation between ENSO 3.4 and the GBS time series.

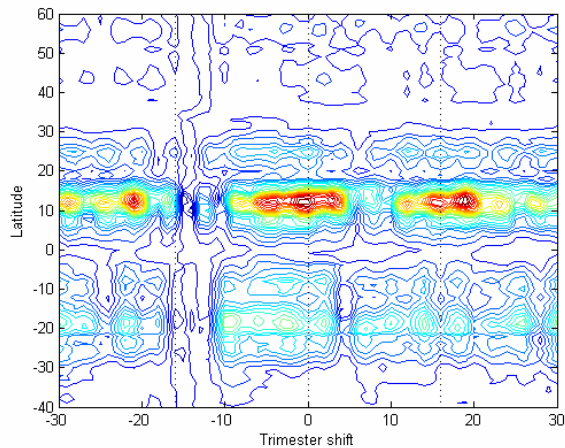


Figure 4. Spatial-temporal inter-correlation between ENSO 1-2 and the GBS time series.

3. RESULTS AND DISCUSSIONS

Fires occur somewhere in our planet every week, if not every day. Figure 1 shows that fire activity is actually a global phenomenon in a perpetual and recurrent process. During the period considered in this work (1982-1999), the global fire activity presents alternated periods of maximum and minimum of activity. Figure 1 clearly depicts a temporal shift (~2 trimesters) between the fire

activity in the northern and southern hemispheres, and between the fire activity in tropical and medium-high latitudes in the northern hemisphere.

Several authors (Swetnam and Betancourt, 1990; Rodo et al., 1997; Malingreau et al., 1995) have found an increase in the frequency and extent of fires at regional scale connected with ENSO events. The results presented in this paper show this connection at global scale at different latitudes and the recurrent behavior of these phenomena during the period considered in this paper.

Figures 3 and 4 show a good correlation between ENSO and GBS time series in two ranges of latitudes (7°N-15°N) and (15°S-20°S). Figure 4 shows noisier correlation values which are probably due to ENSO 1-2 signal characteristics as explained in the precedent paragraph.

Table A. ENSO indices used in this study and the associated regions.

Index	Lat range	Lon range
ENSO 1-2	0°- 10° S	90° – 80° W
ENSO 3.4	5° N – 5° S	170° – 120° W

The range of latitudes (7°N-15°N) corresponds with African Savannahs, North and Centre of Latin America, East of Southern Asia and India. In figures 3 and 4, the main correlation peak for these latitudes is centred on 0. Also for these latitudes, secondary symmetrical peaks come into view at 16-19 trimesters (~4 years) showing a connection between the fire activity and ENSO returns during the period of time considered in this paper.

The other main range of latitudes (15°S-20°S) corresponds with Southern Africa and Madagascar, Southern Brazil, Argentina, Chile and Northern Australia. Here again, inter-correlation peaks (even if noisy) show a good agreement between both phenomena at these latitudes. The temporal shift between both signals is due to the natural shift (~6 months – Carmona-Moreno et al., 2005.a-b) of the fire activity between both hemispheres.

A secondary range of latitudes (20°N-30°N) corresponds with Southern of North America, Mediterranean area, North India, Mongolia and North China. Figure 3 shows noisy correlation values but with clear annual and almost quadrennial (16-20 trimesters) pattern cycles phased with ENSO events during the period of time considered in this paper. This is also visible in figure 4 but with secondary correlation peaks. This is more difficult to interpret and further studies and longer time series of data (> 40 years) are necessary. In the boreal regions, no significant correlations were found between both phenomena.

4. CONCLUSIONS

This paper presents the inter-correlation results obtained from GBS time series with two ENSO indices: ENSO 3.4 and ENSO 1-

2. Clear regular patterns at three ranges of latitudes are detected showing a good agreement between both phenomena during the period of time considered in this paper (1982-1999). Correlations with ENSO 1-2 are noisier but this could be due to the intrinsic characteristics of this signal to represent ENSO events.

From this first analysis, we can conclude that there is a clear connection between the intensity of the global fire activity (measured as the extension of burned surfaces detected from satellite data) and the ENSO events but longer time series (> 40 years) of burned surfaces is needed to confirm these results.

5. REFERENCES

- Arino O., Simon M., Piccolini I., Rosaz J.M., **The ERS-2 ATSR-2 World Fire Atlas and the ERS-2 ATSR-2 World Burnt Surface Atlas Projects**. Proc. 8th ISPRS conference on Physical Measurement and Signatures in Remote Sensing, Aussois, 8-12 January 2001.
- Belward A., Hollifield A., James M. **The potential of the NASA GAC Pathfinder product for the creation of global thematic data sets: the case of biomass burning patterns**. *International Journal of Remote Sensing*, **16**, 11, pp. 2089-2097. (1995)
- Barbosa, P.M., Stroppiana, D. and Gregoire, J.M., An assessment of vegetation fire in Africa (1981-1991). **Burnt areas, burnt biomass and atmospheric emissions**. *International Journal of Global Biogeochemical Cycles* **13**, N4, pp. 933-950. (1999).
- Camberlin P, Janicot S., Pocard I. (2001) **Seasonality and atmospheric dynamics of the teleconnection between African rainfall and tropical ocean surface temperature: Atlantic vs. ENSO**. *International Journal of Climatology*, **21**, pp. 973-1005. 2001.
- Carmona-Moreno C., A. Belward, J.P. Malingreau, A. Hartley, M. Garcia-Alegre, M. Antonovskiy, V. Buchshtaber, V. Pivovarov (2005.a). **Characterising interannual variation in global fire calendar using data from Earth Observing satellites**. *Global Change Biology*. Accepted for publication. March 2005.
- Carmona-Moreno C., A. Belward, J.P. Malingreau, A. Hartley, Ph. Caperan, M. Garcia-Alegre, M. Antonovskiy, V. Buchshtaber, V. Pivovarov (2005.b). **A Burning World. Spatial-temporal analyses of the Global Fire Activity from NOAA-AVHRR time series (1982-1999)**. European Union Report EUR 21477 EN. ISBN 92-894-8800-X. January 2005.
- Crutzen, P.J., Heidt L.E., J.P. Krasnec, Pollock W.H. and Seiler W. **Biomass burning as a source of atmospheric gases CO, H₂, N₂O, NO, CH₃Cl and COS**, *Nature* **282**, pp. 253-256, (1979).
- Dwyer, E., Pinnok, S, and Gregoire, J.-M., **Global spatial and temporal distribution of vegetation fire as determined from satellite observations**. *International Journal of Remote Sensing*, **21**, N^o6&7, pp. 1289-1302 (2000).
- FAO 2001. **FRA Global Forest Fire Assessment 1990-2000**. *Forest Resources Assessment Programme*, Working Paper 55. FAO, Rome, 495 pp.
- Hao, W. M. and M.-H. Liu. **Spatial and temporal distribution of tropical biomass burning**. *Global Biogeochemicals*, **8**, 495-503, 1994.
- Hanley D.E., Bourassa M.A., O'Brien J.J., Smith S.R., Spade E.R., (2003). **A quantitative evaluation of ENSO Indices**. *Journal of Climate*. Vol. 16, pp. 1249-1258, 15 April 2003.
- Innes, J.L., Beniston, M., Verstraete, M.M., **Biomass burning and its inter-relationships with the climate system**. (Kluwer Academic Publisher, The Netherlands, 2000).
- Lyon B. (2004) **The strength of El Niño and the spatial extent of tropical drought**. *Geophysical Research Letters*, vol. 31, L21204, doi: 10.1029/2004GL020901, 2004.
- Malingreau J.P., Stephens G., Fellows L. (1985). **Remote Sensing of Forest Fires: Kalimantan and North Borneo in 1982-83**, *Ambio* **14**, pp. 314-321. 1985.
- Moreno-Ruiz, J.A., Barbosa, P.M., Carmona-Moreno, C., Gregoire, J.M., Belward, A.S., **GLINTS-BS – Global Burn Scar Detection System**. European Union Technical Note **L99.167**. May (1999).
- Payette S. (1992). **Fire as a controlling process in the North American boreal forest**. In A systems analysis of the Global Boreal Forest (edited by H.H. Shugart, R. Leemans and G.B. Bonan published by Cambridge University Press, Cambridge, 1992).
- Rodo, X., Baert, E., and Comin, F.A. (1997). **Variations in seasonal rainfall in Southern Europe during the present century: relationships with the North Atlantic Oscillation and the El Niño-Southern Oscillation**, *Climate Dynamics*, **13**, pp. 275-284. 1997.
- Ropelewski C. F., Halpert M. S., Wang X., **Observed Tropospheric Biennial Variability and Its Relationship to the Southern Oscillation**. *Journal of Climate*, vol. **5**, pp. 594-614 (1992).
- Seiler W. and Crutzen P.J. **Estimates of gross and net fluxes of carbon between the biosphere and the atmosphere from biomass burning**. *Climatic Change*, **2**, pp. 207-247, (1980).
- Sellers, P.J., S.O. Los, C.J. Tucker, C.O. Justice, D.A. Dazlich, G.J. Collatz, and D.A. Randall., **The generation of global fields of terrestrial biophysical parameters from the NDVI**. *International Journal of Remote Sensing*, **15**(7), pp. 3519-3545 (1994).
- Swetnam T.W., Betancourt J.L. (1990). **Fire-Southern Oscillation relations in the Southwestern United States**. *Science*, **249** (31 August), pp. 1017-1020. 1990.
- Tucker, C.J., Fung, I.Y., Keeling, C.D., Gammon, R.H., **Relationship between atmospheric CO₂ variations and satellite-derived vegetation index**. *Nature*, **319**, pp. 195-199. (1986).